Molecular Plant Pathology

MOLECULAR PLANT PATHOLOGY (2018) 19(6), 1377–1390 DOI: 10.1111/mpp.12621

The major leaf ferredoxin Fd2 regulates plant innate immunity in Arabidopsis

MO WANG[1,2,3], LU RUI[2,4], HAOJIE YAN[5], HUA SHI[2,4], WANYING ZHAO[6], JINSHAN ELLA LIN[6,7], KAI ZHANG[1,8], JOSHUA J. BLAKESLEE[6,7], DAVID MACKEY[6], DINGZHONG TANG[2,4], ZHONGMIN WEI[9] AND GUO-LIANG WANG[1,8,*]

[1]*Department of Plant Pathology, Ohio State University, Columbus, OH 43210, USA*

[2]*Key Laboratory of Ministry of Education for Genetics, Breeding and Multiple Utilization of Crops, Plant Immunity Center, Fujian Agriculture and Forestry University, Fuzhou 350002, China*

[3]*Fujian University Key Laboratory for Plant–Microbe Interaction, Fujian Agriculture and Forestry University, Fuzhou 350002, China*

[4]*State Key Laboratory of Ecological Control of Fujian-Taiwan Crop Pests, Fujian Agriculture and Forestry University, Fuzhou 350002, China*

[5]*State Key Laboratory of Plant Cell and Chromosome Engineering, Institute of Genetics and Developmental Biology, Chinese Academy of Sciences, Beijing 100101, China*

[6]*Department of Horticulture and Crop Science, Ohio State University, Columbus/Wooster, OH 43210, USA*

[7]*Department of Horticulture and Crop Sciences, OARDC Metabolite Analysis Cluster (OMAC), Wooster, OH 44691, USA*

[8]*State Key Laboratory for Biology of Plant Diseases and Insect Pests, Institute of Plant Protection, Chinese Academy of Agricultural Sciences, Beijing 100193, China*

[9]*Plant Health Care, Inc., Seattle, WA 98121, USA*

SUMMARY

Ferredoxins, the major distributors for electrons to various acceptor systems in plastids, contribute to redox regulation and antioxidant defence in plants. However, their function in plant immunity is not fully understood. In this study, we show that the expression of the major leaf ferredoxin gene *Fd2* is suppressed by *Pseudomonas syringae* pv. *tomato* (*Pst*) DC3000 infection, and that knockout of *Fd2* (*Fd2-KO*) in Arabidopsis increases the plant's susceptibility to both *Pst* DC3000 and *Golovinomyces cichoracearum*. On *Pst* DC3000 infection, the *Fd2-KO* mutant accumulates increased levels of jasmonic acid and displays compromised salicylic acid-related immune responses. *Fd2-KO* also shows defects in the accumulation of reactive oxygen species induced by pathogen-associated molecular pattern-triggered immunity. However, *Fd2-KO* shows enhanced R-protein-mediated resistance to *Pst* DC3000/*AvrRpt2* infection, suggesting that Fd2 plays a negative role in effector-triggered immunity. Furthermore, Fd2 interacts with FIBRILLIN4 (FIB4), a harpin-binding protein localized in chloroplasts. Interestingly, Fd2, but not FIB4, localizes to stromules that extend from chloroplasts. Taken together, our results demonstrate that Fd2 plays an important role in plant immunity.

Keywords: ferredoxin, fibrillin, harpin, jasmonic acid, reactive oxygen species, salicylic acid, stromule.

* *Correspondence*: Email: wang.620@osu.edu

INTRODUCTION

To defend against a wide range of pathogenic microorganisms in the environment, plants have evolved a sophisticated innate immune system (Jones and Dangl, 2006; Schwessinger and Ronald, 2012). In addition to using preformed physical and chemical barriers, plants mount active responses to protect themselves. One branch of plant immunity, which is activated on recognition of conserved pathogen-associated molecular patterns (PAMPs) by cell surface transmembrane proteins known as pattern recognition receptors, is referred to as PAMP-triggered immunity (PTI) (Yamaguchi *et al.*, 2013). To overcome PTI, pathogens deploy defence-suppressing effector proteins that are secreted into the apoplastic space or are translocated into the host cytoplasm (Chisholm *et al.*, 2006). To counter the activity of the pathogen effectors, plants use resistance (R) proteins that act as intracellular receptors. R proteins perceive pathogen effectors and thereby activate effector-triggered immunity (ETI), which is a rapid and robust response often associated with a hypersensitive response (HR) (Akamatsu *et al.*, 2013; Liu W *et al.*, 2013).

Increasing numbers of studies have indicated that the chloroplast plays an important role in plant immunity (Nomura *et al.*, 2012; de Torres Zabala *et al.*, 2015). Various defence signalling molecules, including reactive oxygen species (ROS), salicylic acid (SA) and jasmonic acid (JA), are synthesized in the chloroplast (Serrano *et al.*, 2016). In addition, the organelle is required for the integration of multiple environmental stimuli and for the active communication of the signals to other organelles (Padmanabhan and Dinesh-Kumar, 2010).

Ferredoxins (Fds), a group of small iron–sulfur [2Fe–2S] cluster-containing proteins, are soluble electron carriers that distribute electrons from photosystem I (PSI) to the various acceptor systems of metabolic processes in the chloroplast stroma (Hanke

and Mulo, 2013). Fd1 and Fd2 are the photosynthetic and leaf-localized Fds in Arabidopsis (Hanke and Hase, 2008). Fd2, which constitutes about 90% of the total leaf Fd complement, functions in linear photosynthetic electron transport; the less abundant Fd1 has been implicated in cyclic electron flow (Hanke *et al.*, 2004). A previous study has found that the *Fd2*-knockout mutant (*Fd2-KO*) of Arabidopsis accumulates increased levels of ROS in the chloroplast, possibly because of the excess electrons transferred from PSI to O_2 (Voss *et al.*, 2008). Another study has reported that *Fd2-KO* plants exhibit greater adaptation than wild-type (WT) plants to long-term high-light conditions through the up-regulation of photoprotection-related genes (Liu J *et al.*, 2013). In addition, transplastomic tobacco expressing *Fd2* in its chloroplasts shows increased tolerance to abiotic stresses, and especially to low-light conditions (Yamamoto *et al.*, 2006).

FIBRILLIN4 (FIB4) is a thylakoid membrane- and plastoglobule-localized protein that associates with the photosystem II (PSII) light-harvesting complex (Friso *et al.*, 2004; Galetskiy *et al.*, 2008; Peltier *et al.*, 2004; Vidi *et al.*, 2006; Ytterberg *et al.*, 2006). The *fib4* knockdown apple tree mutant and Arabidopsis *fib4* mutant are more susceptible than WT plants to bacterial pathogens (Singh *et al.*, 2010). Recently, FIB4 has been found to be required for a high level of accumulation of plastoquinone in the plastoglobule (Singh *et al.*, 2012). In addition, FIB4 interacts with the harpin protein, HrpN (Song *et al.*, 2002). Harpins are glycine-rich, cysteine-lacking and heat-stable proteins secreted via Type III secretion by Gram-negative plant-pathogenic bacteria (Choi *et al.*, 2013; Wei *et al.*, 1992). HrpN, the founder protein of the harpin family, is secreted by *Erwinia amylovora* and was the first pathogen-independent HR elicitor characterized in plants (Wei *et al.*, 1992).

Fds can enhance harpin-mediated HR in plants. For example, PFLP, which is the Fd from sweet pepper, increases ROS generation and enhances the HR in tobacco in response to harpin treatments (Dayakar *et al.*, 2003). Furthermore, overexpression of the sweet pepper *PFLP* gene in transgenic Arabidopsis activates HR-associated events and increases resistance to *Erwinia carotovora* ssp. *carotovora* (*ECC*), but not to its harpin mutant strain. These results suggest that high levels of ectopic PFLP may lead to the recognition of the harpin and to the activation of the HR and other defence responses (Ger *et al.*, 2014). However, the exact function of Fd in plant immune responses is still unclear.

In this study, we found that Arabidopsis Fd2 plays an important role in immune resistance to *Pseudomonas syringae* pv. *tomato* (*Pst*) DC3000 and *Golovinomyces cichoracearum* via the suppression of innate JA accumulation and regulation of PTI. Fd2 interacts with FIB4, and the expression of both genes increases in response to harpin treatment. In addition, Fd2 is localized in the stromules, which suggests that it might function in retrograde signal transduction. These results provide new insights into the mechanisms of Fd2-mediated innate immunity in plants.

RESULTS

Knockout of *Fd2* increases susceptibility to the pathogens

To investigate the role of the major leaf Fd in plant innate immunity, we first quantified the expression level of *Fd2* in Arabidopsis following infection by the virulent hemibiotrophic bacterium *Pst* DC3000. Within 12 h post-infection (hpi), transcription of *Fd2* was not significantly different between plants inoculated with buffer alone (control) and the bacterium (Fig. 1a, left). At 24 and 48 hpi, however, *Fd2* transcript levels in bacterium-inoculated plants were markedly lower than in control plants and also significantly lower than at 0 and 12 hpi (Fig. 1a, left). Unlike *Fd2*, *FIB4* transcripts were not significantly affected by *Pst* DC3000 infection (Fig. 1a, right). We also performed immunoblot analysis using protein isolated from Col-0 before and after infection with the polyclonal antibody generated against plant Fd (FDX1). Consistent with the transcription data, the Fd2 protein level was reduced at 2 days post-infection (dpi) in Col-0 (Fig. S1a,b, see Supporting Information). Taken together, these results demonstrate that *Pst* DC3000 infection reduces the expression of *Fd2*, but not *FIB4*, in Arabidopsis.

Next, we inoculated an *Fd2-KO* mutant (Voss *et al.*, 2008) and its WT background, Nossen, with *Pst* DC3000 by infiltration. At 4 dpi, bacterial speck disease symptoms were more severe on *Fd2-KO* than on WT plants (Fig. 1b, left panel). Bacterial counts indicated that *Fd2-KO* supported significantly more *Pst* DC3000 growth than WT (Fig. 1b, right panel). We also challenged *Fd2-KO* mutant and WT plants with a virulent biotrophic powdery mildew *G. cichoracearum* strain (UCSC1), followed by quantification of conidiophore formation. The inoculation analysis showed that the *Fd2-KO* mutant also displayed more susceptibility than the WT (Fig. 1c). Therefore, our results demonstrate that Fd2 is required for resistance against both the hemibiotrophic pathogen *Pst* DC3000 and the biotrophic pathogen *G. cichoracearum*.

The *Fd2-KO* mutant displays reduced PTI-induced ROS accumulation

To determine why *Fd2-KO* is more susceptible to pathogen infection, we assessed whether the PTI pathway is affected by the absence of Fd2. We first measured the ROS burst in response to treatments with the PAMPs, flg22 and chitin, in *Fd2-KO* and WT. Although ROS accumulation was detected in both *Fd2-KO* and WT, ROS levels were lower in *Fd2-KO* than in WT at all time points (Fig. 2a). Next, we analysed the transcriptional levels of two plasma membrane-bound NADPH oxidases, *AtrbohD* and *AtrbohF*, that are required for apoplastic ROS accumulation (Torres *et al.*, 2002). Consistent with the reduced ROS accumulation in response to PAMP treatments, *Fd2-KO* displayed lower levels of both

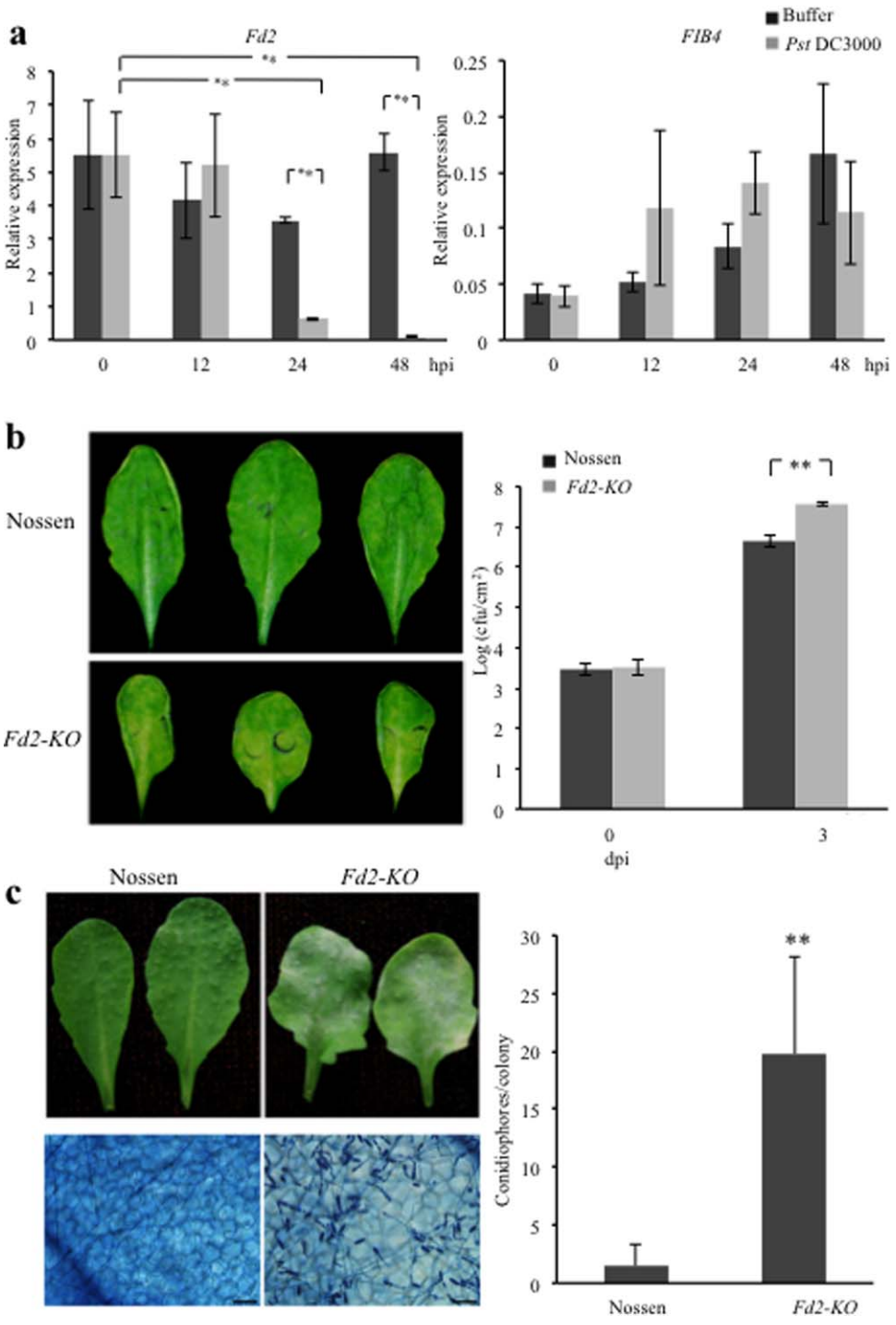

AtrbohD and *AtrbohF* transcripts than WT in the absence of any treatment (Fig. 2b). We also determined the transcriptional levels of *FLG22-INDUCED RECEPTOR-LIKE KINASE 1* (*FRK1*), a marker gene of late PTI responses (Asai *et al.*, 2002). As shown in Fig. 2c, *FRK1* transcription did not differ significantly between *Fd2-KO* and WT before inoculation. After inoculation with *Pst* DC3000, *FRK1* transcription was strongly induced in both *Fd2-KO* and WT; however, transcript levels were lower in *Fd2-KO* than in WT, particularly at 2 dpi, when *FRK1* transcript levels continued to increase in WT, but began to decline in *Fd2-KO* (Fig. 2c). Based on these results, we conclude that Fd2 is involved in the regulation of PTI responses.

Fig. 1 The *Fd2*-knockout mutant (*Fd2-KO*) exhibits increased susceptibility to pathogen infection. (a) After infiltration inoculation with *Pseudomonas syringae* pv. *tomato* (*Pst*) DC3000 [optical density at 600 nm (OD_{600}) = 0.0002] or 10 mM $MgCl_2$ as the control, total RNA was extracted from the inoculated leaves of 4-week-old Col-0 plants at the indicated time points. The relative transcriptional levels of *FIB4* and *Fd2* were determined by quantitative real-time polymerase chain reaction (qRT-PCR). The transcription of *Fd2* (left), but not *FIB4* (right), was down-regulated by *Pst* DC3000 at 24 and 48 h post-infection (hpi). All qRT-PCR assays were performed with *Actin* as the endogenous control. Error bars represent the standard deviation (SD) ($n = 3$) from three biological repeats, and the significance was determined at $^{**}P < 0.01$ with Student's *t*-test. (b) Four-week-old Nossen and *Fd2-KO* plants were infected with *Pst* DC3000 ($OD_{600} = 0.0002$) by infiltration. Inoculated leaves at 4 days post-infection (dpi) are shown on the left, and bacterial numbers at 0 and 3 dpi are indicated on the right. cfu, colony-forming units. Error bars represent the SD ($n = 3$) from three biological repeats, and the significance was determined at $^{**}P < 0.01$ with Student's *t*-test. (c) Four-week-old Nossen and *Fd2-KO* plants were inoculated with *Golovinomyces cichoracearum*. The infected leaves were photographed at 8 dpi (left top). Fungal growth, as indicated by staining with trypan blue, is shown on the left bottom. Bar, 50 μm. Fungal growth in plants at 5 dpi, as indicated by the number of conidiophores per colony, is shown on the right. The bars represent the mean and SD; significance was determined at $^{**}P < 0.01$ with a one-way analysis of variance. All results in this figure are from one of three independent experiments performed with similar results.

The *Fd2-KO* mutant accumulates high levels of JA in response to *Pst* DC3000 infection

To determine whether the biosynthesis of defence-related hormones is affected by the absence of Fd2, we quantified the levels of SA, JA and JA-isoleucine/leucine (JA-Ile/Leu) in *Pst* DC3000-infected *Fd2-KO* and WT plants with buffer infiltration as a control via high-performance liquid chromatography-tandem mass spectroscopy (LC-MS/MS). Because of the transient nature of increases in phytohormone concentrations following stress stimuli, these experiments were repeated three times, with each study containing three to five biological replicates. In all cases, the *Fd2-KO* mutant accumulated significantly higher levels of JA and JA-Ile/

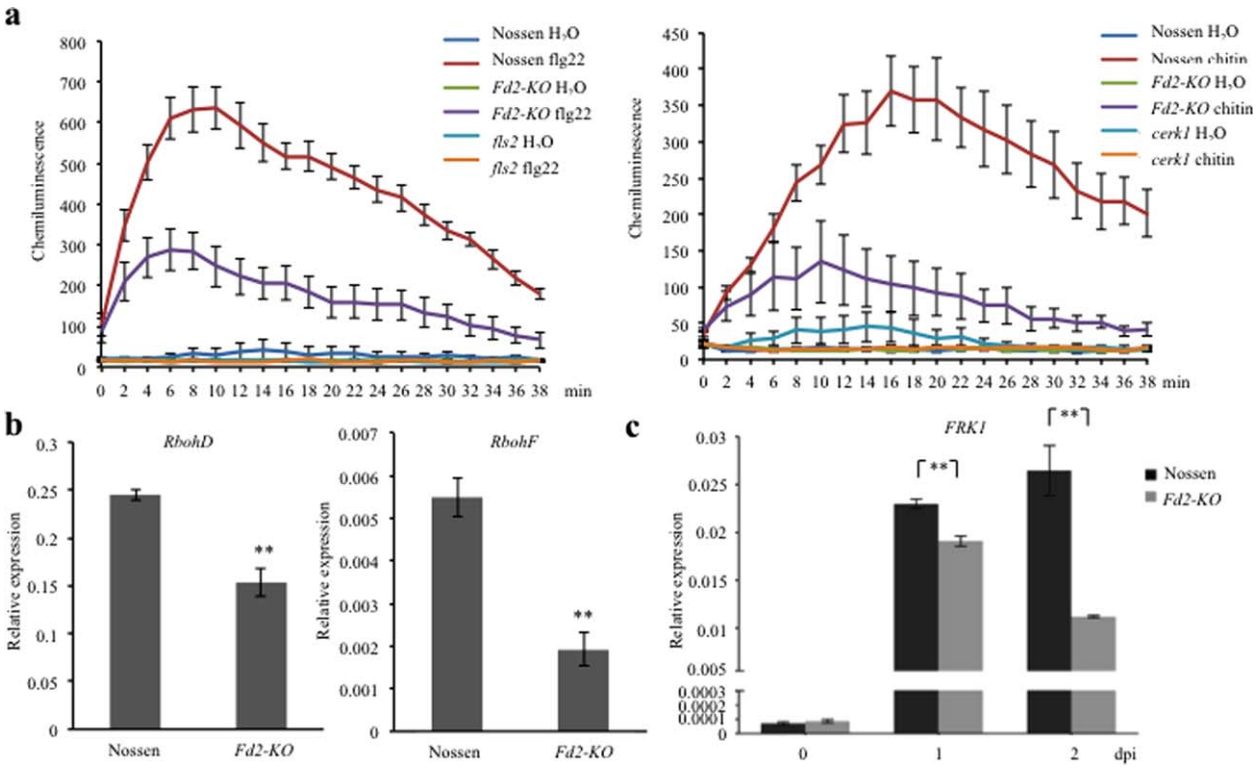

Fig. 2 The *Fd2*-knockout mutant (*Fd2-KO*) is defective in pathogen-associated molecular pattern (PAMP)-triggered immunity (PTI)-induced reactive oxygen species (ROS) accumulation. (a) To detect ROS, leaf strips of Nossen and *Fd2-KO* plants were treated with 100 nM flg22 (left) or 200 μg/mL chitin (right) in buffer containing luminol and horseradish peroxidase. Luminescence was recorded at the indicated times. *fls2* and *cerk1* mutants were used as negative controls for flg22 and chitin treatment, respectively. Error bars represent the standard error (SE) ($n = 8$). (b) The relative transcriptional levels of *RbohD* (left) and *RbohF* (right) in 4-week-old non-treated Nossen and *Fd2-KO* plants as determined by quantitative real-time polymerase chain reaction (qRT-PCR). (c) The induction of *FRK1* as indicated by qRT-PCR in Nossen and *Fd2-KO* plants before and after *Pseudomonas syringae* pv. *tomato* (*Pst*) DC3000 [optical density at 600 nm (OD_{600}) = 0.0002] inoculation. In (b) and (c), *Actin* was used as the endogenous control; significance was determined at $^{**}P < 0.01$ with Student's *t*-test, and error bars represent SE ($n = 3$). Experiments were conducted in triplicate with similar results. dpi, days post-infection.

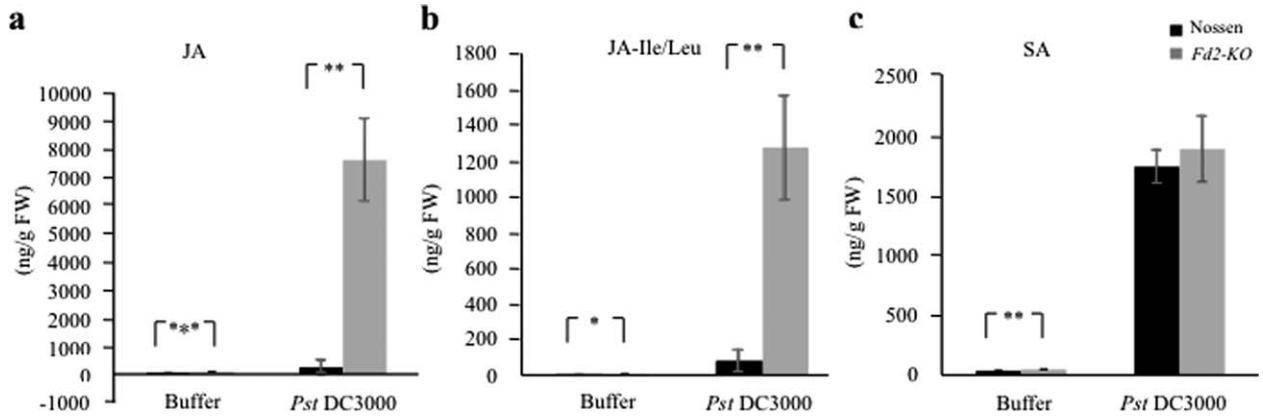

Fig. 3 The *Fd2*-knockout mutant (*Fd2-KO*) accumulates high levels of jasmonic acid (JA) and JA-isoleucine/leucine (JA-Leu/Ile) in response to pathogen infection. Four-week-old Nossen and *Fd2-KO* plants were inoculated with *Pseudomonas syringae* pv. *tomato* (*Pst*) DC3000 [optical density at 600 nm (OD_{600}) = 0.001] or buffer (10 mM $MgCl_2$) by leaf infiltration. At 2 days post-infection (dpi), samples were collected for JA (a), JA-Ile/Leu (b) and salicylic acid (SA) (c) quantification. Significance was determined using Student's *t*-test (two-tailed, type III, unequal variance); $*P < 0.05$, $**P < 0.01$ and $***P < 0.001$. Error bars represent the standard deviation (SD) ($n = 5$ for all samples, except that $n = 4$ for *Pst* DC3000-treated *Fd2-KO*). The experiment was repeated three times, and representative results are shown. FW, fresh weight.

Leu than WT following inoculation with *Pst* DC3000 (2 dpi; Fig. 3a,b). The increase in JA levels in *Fd2-KO* post-infection was dramatic (over 90-fold increases in most experiments conducted), particularly because WT showed no significant increase in JA accumulation at 2 dpi (Fig. 3a). A similar trend was observed with JA-Ile/Leu, whose levels post-infection were significantly higher in *Fd2-KO* than in WT (Fig. 3b). As with JA levels, JA-Ile/Leu levels in WT plants showed no significant increase at 2 dpi. Interestingly, loss of Fd2 might also result in increased resting levels of JA and JA-Ile/Leu, although this trend was not consistent across all experiments, perhaps because of their low levels in the leaves of control plants. In addition, infection increased levels of SA in both *Fd2-KO* and WT plants, but SA levels did not differ significantly between the mutant and WT post-infection (Fig. 3c). Together, these results demonstrate that a loss of Fd2 leads to the generation of high levels of JA and JA-Ile/Leu in response to *Pst* DC3000 infection, but does not affect SA accumulation.

The induction of SA-responsive defence genes is defective in *Fd2-KO* in response to *Pst* DC3000 infection

Based on the differences in JA and JA-Ile/Leu levels in *Fd2-KO* vs. WT plants and on the potential interactions between the JA and SA signalling pathways, we measured the expression level of genes in both JA- and SA-mediated immunity pathways. First, we analysed the transcription of *PDF1.2*, a JA-responsive gene involved in defence against necrotrophic pathogens (Penninckx *et al.*, 1998). In WT, inoculation with *Pst* DC3000 increased *PDF1.2* transcript levels at 1 dpi and, to a lesser extent, at 2 dpi. Consistent with the high JA and JA-Ile/Leu levels in *Fd2-KO* after infection, *PDF1.2* transcripts accumulated to a significantly higher level in *Fd2-KO* than in WT at both 1 and 2 dpi (Fig. 4a). MYC2 is a JA-responsive transcription factor that plays a key role in the regulation of cross-talk between SA and JA (Lorenzo *et al.*, 2004; Thaler *et al.*, 2012). *SID2* (also known as *ICS1*) encodes an isochorismate synthase that is required for the synthesis of SA from chorismate for plant defence (Wildermuth *et al.*, 2001). MYC2 can activate the expression of the NAC transcription factor genes, which, in turn, reduce the expression of *SID2* (Zheng *et al.*, 2012). We found that *MYC2* transcript levels were significantly higher in *Fd2-KO* than in WT before and at 1 dpi with *Pst* DC3000, and were similar in both genotypes at 2 dpi (Fig. 4b). *SID2* transcript levels were significantly lower in *Fd2-KO* than in WT before and at 1 dpi with *Pst* DC3000, and were similar in both genotypes at 2 dpi (Fig. 4c). This inverse relationship between the levels of *MYC2* and *SID2* transcripts before and after *Pst* DC3000 infection correlates with the *MYC2*-dependent reduction of *SID2* expression.

We also quantified the transcripts of SA-responsive genes in *Fd2-KO* and WT following *Pst* DC3000 infection. Interestingly, although SA accumulation was not affected, the transcript levels of *PR1*, *PR2* and *PR5* were reduced before and after infiltration with *Pst* DC3000 in *Fd2-KO* plants (Fig. 4d–f). *NPR1* encodes a transcription cofactor and is required for SA-induced transcription of *PR* genes (Zhang *et al.*, 1999). EDS5 localizes to the chloroplast envelope and exports SA from chloroplast to cytoplasm (Serrano *et al.*, 2013). Consistent with the patterns of hormone accumulation and gene expression, the transcript levels of both *NPR1* and *EDS5* were significantly lower in *Fd2-KO* than in WT before and after *Pst* DC3000 infection (Fig. S2a,b, see Supporting Information). Taken together, our data indicate that the higher accumulation of JA and JA-Ile/Leu in the absence of Fd2 activates the JA

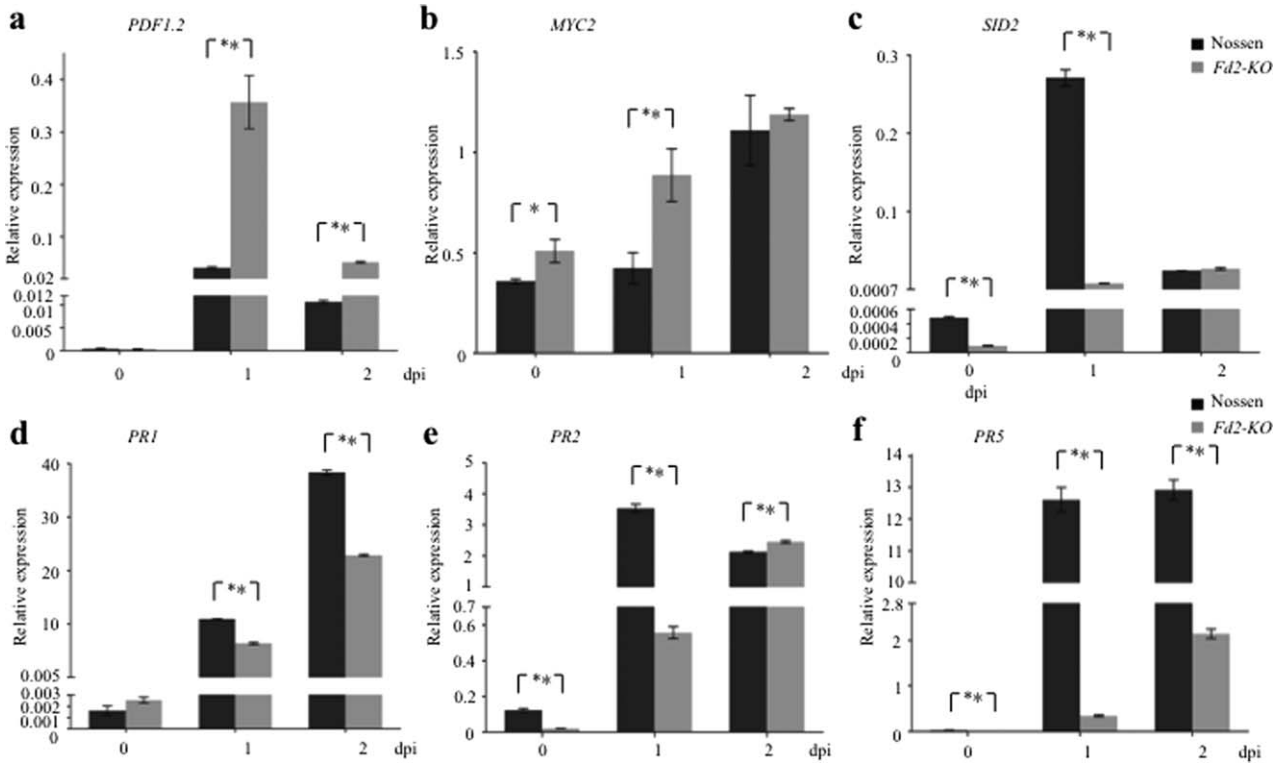

Fig. 4 The *Fd2*-knockout mutant (*Fd2-KO*) displays enhanced expression of jasmonic acid (JA)-responsive genes and compromised induction of salicylic acid (SA)-responsive genes on pathogen infection. After inoculation with *Pseudomonas syringae* pv. *tomato* (*Pst*) DC3000 [optical density at 600 nm (OD_{600}) = 0.0002] by infiltration, total RNA was extracted from the inoculated leaves of Nossen and *Fd2-KO* plants at the indicated times. The relative transcriptional levels of *PDF1.2* (a), MYC2 (b), *SID2* (c), *PR1* (d), *PR2* (e) and *PR5* (f) were determined by quantitative real-time polymerase chain reaction (qRT-PCR) with *Actin* as the endogenous control. Error bars represent the standard error (SE) ($n = 3$), and significance was determined at $^*P < 0.05$ and $^{**}P < 0.01$ with Student's *t*-test. Experiments were conducted in triplicate with similar results. dpi, days post-infection.

signalling pathway, which may, in turn, suppress the SA signalling pathway after pathogen infection.

Fd2 negatively regulates Rps2-mediated ETI

To investigate the role of Fd2 in ETI, we inoculated *Fd2-KO* and WT plants with *Pst* DC3000 containing *avrRpt2* and *avrRpm1*, whose products are recognized by the corresponding nucleotide-binding oligomerization domain- and leucine-rich repeat-containing proteins, RPS2 and RPM1, respectively (Axtell and Staskawicz, 2003; Mackey *et al.*, 2002). The non-pathogenic *Pst* DC3000 strain with deletion of the *hrcC* gene (*Pst* DC3000/Δ*hrcC*), which is required for effector secretion, was used as the control. The inoculation assay showed that *Fd2-KO* displayed enhanced resistance against *Pst* DC3000/*avrRpt2*, because the bacterial growth was less in *Fd2-KO* than in WT (Fig. 5a). However, the resistance to *Pst* DC3000/*avrRpm1* or *Pst* DC3000/Δ*hrcC* did not differ significantly between *Fd2-KO* and WT (Fig. 5a). We then used 3,3-diaminobenzidine tetrahydrochloride (DAB) staining to quantify H_2O_2 accumulation in *Fd2-KO* and WT on *Pst* DC3000/*avrRpt2* infection. Consistent with its enhanced resistance, *Fd2-KO* accumulated higher H_2O_2 levels than WT in response to *Pst* DC3000/*avrRpt2* inoculation (Fig. 5b). These results suggest that the *Fd2* mutation enhances *Rps2*-mediated resistance to *Pst* DC3000/*avrRpt2* and causes increased H_2O_2 accumulation.

Fd2 interacts with the hrpN-binding protein FIB4

Because Fd is related to harpin-mediated responses in plants and FIB4 is a harpin-binding protein localized in chloroplasts (Dayakar *et al.*, 2003; Song *et al.*, 2002), we determined the relationship between Fd and FIB4. To investigate whether Fd interacts with FIB4, we first fused the two leaf Fds (Fd1 and Fd2) and FIB4 with glutathione *S*-transferase (GST) and maltose-binding protein (MBP), respectively. The GST-Fd2 protein, but not GST-Fd1 or GST, strongly bound to MBP-FIB4, as revealed by anti-MBP immunoblotting in an *in vitro* pull-down assay (Fig. 6a). Next, we performed a co-immunoprecipitation (co-IP) assay following transient expression of *Fd2-GFP* and *FIB4-HA* in *Nicotiana benthamiana* leaves with the *green fluorescent protein* gene (*GFP*) and *FIB4-HA* co-expression as a negative control. After total protein had been extracted, samples were immunoprecipitated with

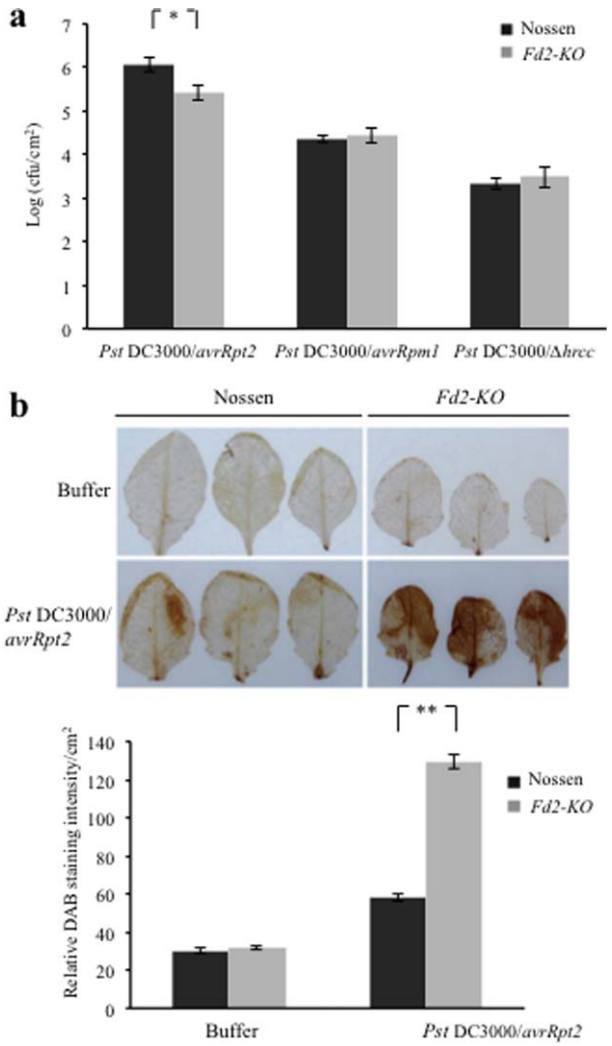

Fig. 5 The *Fd2*-knockout mutant (*Fd2-KO*) is more resistant than Nossen to *Pseudomonas syringae* pv. *tomato* (*Pst*) DC3000/*avrRpt2*. (a) Four-week-old Nossen and *Fd2-KO* plants were infiltration inoculated with *Pst* DC3000/*avrRpt2*, *Pst* DC3000/*avrRpm1* or *Pst* DC3000/Δ*hrcc* [optical density at 600 nm (OD_{600}) = 0.0002]. Bacteria were counted at 3 days post-infection (dpi). cfu, colony-forming units. Error bars represent the standard deviation (SD) ($n = 3$), and significance was determined at $^*P < 0.05$ with Student's *t*-test. Experiments were conducted in triplicate with similar results. (b) Four-week-old Nossen and *Fd2-KO* plants were spray inoculated with *Pst* DC3000/*avrRpt2* ($OD_{600} = 0.2$) or with 10 mM $MgCl_2$ buffer as the control. H_2O_2 production at 10 h after spraying was visualized by 3,3-diaminobenzidine tetrahydrochloride (DAB) staining (top). The relative DAB staining intensity/cm^2 is shown at the bottom. Error bars represent the standard error (SE) ($n = 3$).

anti-GFP antibody. Anti-haemagglutinin (anti-HA) immunoblotting indicated that FIB4-HA was co-immunoprecipitated from the leaves co-expressing both Fd2-GFP and FIB4-HA, but not from the leaves co-expressing GFP and FIB4-HA (Fig. 6b), indicating that Fd2 and FIB4 can form a protein complex *in planta*. We then used the split-luciferase complementation assay to verify the interaction between Fd2 and FIB4 *in planta* (Chen *et al.*, 2008). After the C-termini of Fd2 and FIB4 had been fused with the N-terminal (nLuc) and C-terminal (cLuc) halves of luciferase, respectively, the constructs were transiently co-expressed in *N. benthamiana* leaves. The complemented luciferase activity was detected with the combination of Fd2-nLuc and FIB4-cLuc, but not with the negative controls, nLuc and FIB4-cLuc or Fd2-nLuc and cLuc (Fig. 6c). To determine protein expression, we performed an immunoblotting assay with anti-cLuc antibody to quantify the protein levels of FIB4-cLuc in the leaves co-expressing Fd2-nLuc and FIB4-cLuc or nLuc and FIB4-cLuc (Fig. S3, see Supporting Information). In addition, the binding between FIB4 and HrpN was confirmed by pull-down and co-IP assays (Fig. S4a,b, see Supporting Information). Together, these results indicate that Fd2 interacts with the HrpN-binding protein FIB4 *in vitro* and *in vivo*.

To determine the regulatory relationship between Fd2 and FIB4, we quantified the transcript levels of *FIB4* and *Fd2* in *Fd2-KO* and *fib4-1*, respectively. The analysis showed that levels of *FIB4* transcripts were significantly lower in *Fd2-KO* than in WT Nossen (Fig. S5a, see Supporting Information), suggesting that Fd2 positively regulates *FIB4* expression. However, the levels of *Fd2* transcript were significantly higher in *fib4-1* than in WT Col-0 (Fig. S5b), suggesting that plants may compensate for the *FIB4* mutation by inducing *Fd2*.

To study the expression pattern of *FIB4* and *Fd2* in plants after HrpN treatment, we sprayed 5 μg/mL GST-HrpN onto 4-week-old Col-0 plants, with GST as the control, and determined the transcript levels of *FIB4* and *Fd2* before and at 12 and 24 h after treatment. The analysis indicated that, relative to treatment with GST, GST-HrpN increased *Fd2* expression at 12 and 24 h after treatment and slightly increased *FIB4* transcription at 12 h after treatment (Fig. S6a,b, see Supporting Information). These results demonstrate that HrpN causes accumulation of both *FIB4* and *Fd2* transcripts.

Fd2 is localized in stromules that extend from the chloroplast

We confirmed the chloroplast localization of Fd2 and FIB4 in the protoplasts isolated from *N. benthamiana* leaves that transiently expressed Fd2-GFP or FIB4-GFP (Fig. S7, see Supporting Information). Interestingly, Fd2-GFP localized to stromules extending from the chloroplast (Fig. 7a, top). Some stromules with Fd2-GFP signals were projected to the nuclei, in which weak signals of Fd2-GFP were observed (Fig. 7a, top). As indicated by staining with the nuclear marker 4′,6-diamidino-2-phenylindole (DAPI), Fd2-GFP was in the nucleus that was associated with stromules (Fig. 7b). To exclude the possibility that the observed Fd2-GFP signals were generated by free GFP (i.e. GFP tag cleaved from the Fd2-GFP fusion protein), immunoblotting with anti-GFP antibody was

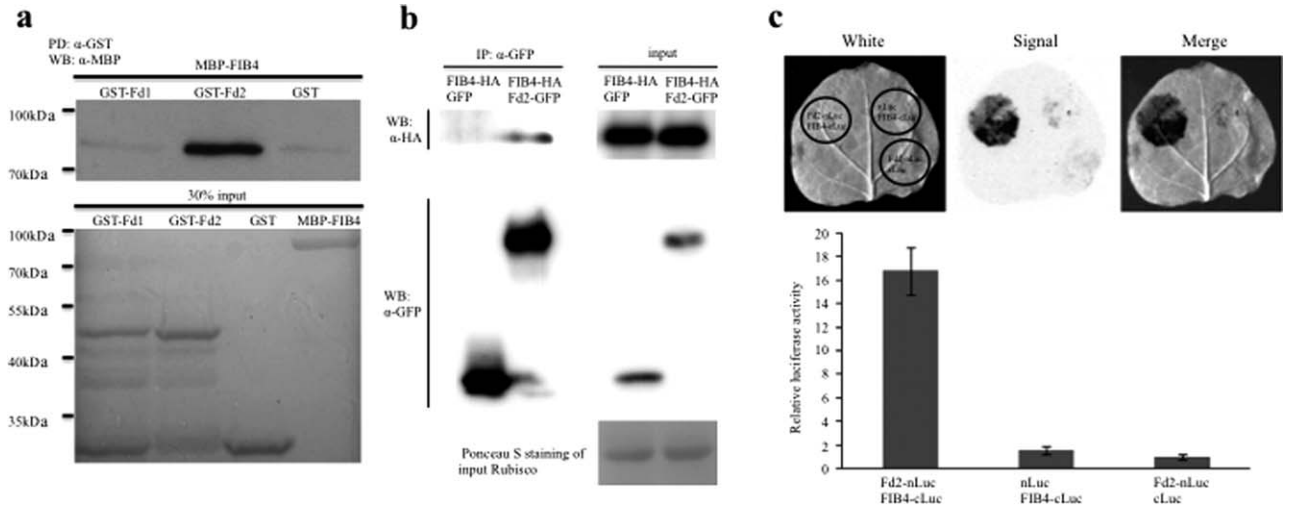

Fig. 6 Fd2 interacts with the HrpN-binding protein FIBRILLIN4 (FIB4). (a) Fd2, but not Fd1, interacts with FIB4 *in vitro*. Purified GST-Fd1, GST-Fd2 and glutathione *S*-transferase (GST) were bound to glutathione resin beads and incubated with purified maltose-binding protein (MBP)-FIB4. After the preparation had been washed, the *in vitro* interaction of MBP-FIB4 with GST-Fd2 was detected by western blotting with α-MBP antibody (top); 30% of the input was loaded and the sample amounts were shown by Coomassie blue staining (bottom). (b) Fd2 also interacts with FIB4 *in vivo*. FIB4-HA and Fd2-GFP were co-expressed in *Nicotiana benthamiana* by agroinfiltration, with FIB4-haemagglutinin (HA) and green fluorescent protein (GFP) co-expression as the control. Proteins were extracted 3 days after infiltration, and immunoprecipitation was carried out with anti-GFP antibody (left). The input is shown on the right. (c) Split-luciferase complementation assays verified the interaction of Fd2 and FIB4. The left half of the *N. benthamiana* leaf was co-infiltrated with Fd2-nLuc/FIB4-cLuc. The right half of the leaf was co-infiltrated with nLuc/FIB4-cLuc and Fd2-nLuc/cLuc as a control. After 2 days of incubation, the inoculated leaves were sprayed with luciferin and chemiluminescence images were captured; the images are shown at the top. The relative luciferase activity values are indicated at the bottom; error bars represent the standard error (SE) ($n = 10$).

carried out using total protein extracted from the *N. benthamiana* leaf tissues transiently expressing Fd2-GFP. As shown in Fig. S8 (see Supporting Information), no free GFP was detected. It follows that the signals in stromules and nuclei were from the Fd2-GFP fusion protein. In contrast with Fd2-GFP, FIB4-GFP was not detected in the stromules or the nucleus (Fig. 7a, bottom). Therefore, our results demonstrate that Fd2 localizes to stromules of the chloroplast and possibly enters into the nucleus via stromules.

DISCUSSION

In this study, we analysed the functions of the primary Fd in Arabidopsis leaves, Fd2, in plant innate immunity. We found that loss of Fd2 causes strong JA and JA-Ile/Leu accumulation on *Pst* DC3000 infection and reduces the expression of the genes in the SA signalling pathway, leading to enhanced susceptibility to *Pst* DC3000 and *G. cichoracearum*. Fd2 also plays a positive role in PTI-mediated ROS accumulation, but negatively regulates the Rps2-mediated ETI response. In addition, Fd2 interacts with the HrpN-binding protein, FIB4, and expression of both *Fd2* and *FIB4* is induced by HrpN treatment. Furthermore, we found that Fd2 is a stromule-localized protein and may be involved in the retrograde signalling pathway. Together, our results provide new insights into a role of Fd2, and more generally of the chloroplast, in the regulation of the plant immune responses.

Fd2 inhibits the accumulation of JA and its amino acid conjugate in response to infection

JA is associated with defence responses against necrotrophic pathogens and herbivorous insects (Glazebrook, 2005), whereas SA contributes to immune responses against biotrophic and hemibiotrophic pathogens (Vlot *et al.*, 2009). The SA and JA defence pathways are often antagonistic to one another (Bari and Jones, 2009). The biosynthesis of JA, a lipid-derived hormone, is initiated in the chloroplasts, but is completed in the peroxisome, and the final chloroplastic intermediate in JA biosynthesis is *cis*-(+)-12-oxophytodienoic acid (OPDA) (Wasternack and Hause, 2013). OPDA is derived from oxidatively modified polyunsaturated fatty acids which, together with JA and methyl JA (MeJA), are collectively termed oxylipins (Howe and Schilmiller, 2002). A previous study has shown that knockout of the key components of the chloroplast photoprotection system in Arabidopsis produces high levels of JA and its precursor OPDA (Demmig-Adams *et al.*, 2013). Similarly, in the absence of Fd2, excess electrons generated from PSI are transferred to O_2, leading to the formation of superoxide (O_2^-), which could also cause lipid peroxidation. The formation of oxylipin hormones resulting from elevated lipid peroxides in the chloroplast may explain why the *Fd2-KO* mutant accumulates more JA and JA-Ile/Leu than WT following *Pst* DC3000 infection. Furthermore, although SA accumulates to the same level in WT

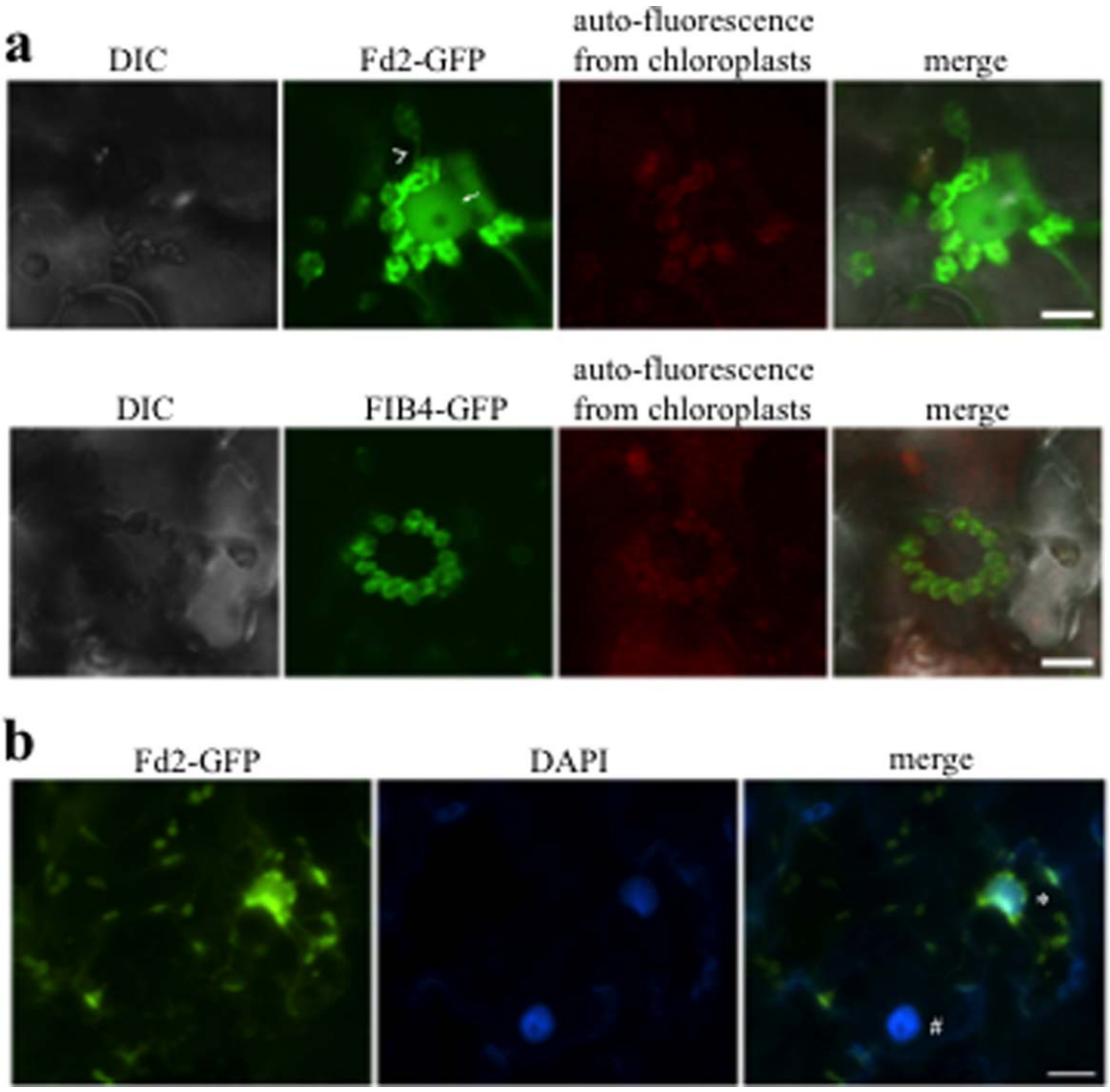

Fig. 7 Fd2 localizes in stromules that extend from chloroplasts. (a) Confocal images of chloroplasts around the nuclei in *Nicotiana benthamiana* cells transiently expressing Fd2-GFP (top) and FIB4-GFP (bottom). Fd2, but not FIBRILLIN4 (FIB4), was found in stromules (top, indicated by arrowheads). A weak Fd2-GFP signal was detected in the nucleus that was associated with the stromules (indicated by arrow). GFP, green fluorescent protein. (b) 4′,6-Diamidino-2-phenylindole (DAPI) was used to visualize the nuclei. The nuclei that were connected with stromules showed strong Fd2-GFP signals (indicated by *), whereas the nuclei without stromules attached showed very weak Fd2-GFP signals (indicated by #). Bars, 10 μm (a) and 20 μm (b). DIC, Differential Interference Contrast.

and *Fd2-KO* in the absence of pathogen attack, the induction of SA-related genes is compromised in the *Fd2-KO* mutant relative to WT on *Pst* DC3000 infection, which may result from the increased JA and JA-Ile/Leu levels in the mutant. Researchers have recently reported that knockout of the gene encoding Arabidopsis NADPH-dependent thioredoxin reductase C (NTRC) which, working together with peroxiredoxin, plays an important role in the chloroplast redox detoxification system, causes a strong increase in JA and JA-Ile content and enhances disease susceptibility (Ishiga *et al.*, 2016). Like the *Fd2-KO* mutant in our study, the *ntrc* mutant showed no defects in SA accumulation, but reduced *SID2* and *PR1* transcription on infection.

RPS2-mediated ETI is compromised in plants unable to accumulate SA (Clarke *et al.*, 2000; Tao *et al.*, 2003). Given our finding that *Fd2-KO* plants show elevated JA accumulation and signalling and reduced SA signalling, it was surprising to find enhanced RPS2-mediated ETI in *Fd2-KO*. However, a recent study has shown that JA enhances RPS2-mediated ETI, although the exact mechanism is unclear (Liu *et al.*, 2016). Therefore, we propose that the resistance of *Fd2-KO* to *Pst* DC3000/*avrRpt2* is indirectly mediated by the high accumulation of JA in the absence of Fd2.

The oxidative burst, a hallmark of PTI responses, is accompanied by a biphasic accumulation of ROS. The first phase, occurring within 1 h following infection, is mostly an apoplastic

accumulation that is tightly linked to NADPH oxidase activity; the second ROS burst, which occurs several hours after infection, is specific to pathogen attack and correlates with ETI and the HR (Shapiguzov *et al.*, 2012; Stael *et al.*, 2015). Growing evidence has indicated that chloroplasts play a crucial role in the second phase of ROS accumulation (Serrano *et al.*, 2016). Increased ROS levels derived from ETI were found to compromise PSII efficiency, which leads to the progressive reduction in the plastoquinone pools involved in the transfer of electrons from PSII to PSI (Mur *et al.*, 2010). In this case, Fd2 could be the reservoir to receive and distribute the extra electrons from PSI. When Fd2 is absent, these overproduced electrons will be transferred to O_2, forming H_2O_2. This may explain why the *Fd2-KO* mutant displays enhanced ROS accumulation on ETI activation.

Functions of Fd2 in the mediation of the harpin-induced responses

Although the harpin protein was discovered over 20 years ago (Wei *et al.*, 1992), the mechanism underlying harpin-induced resistance and the HR is still not clear. In tobacco leaves, harpin infiltration causes the redistribution of chloroplasts in the palisade mesophyll cells and modification of the thylakoid membrane structure, which are early hallmarks of plant HR (Boccara *et al.*, 2007). Thus, chloroplasts may be important in harpin-induced plant responses. In addition, small amounts of HrpN are translocated into plant cells infected by *E. amylovora* (Bocsanczy *et al.*, 2008). We found that the transient expression of HrpN in *N. benthamiana* by agroinoculation induced a weak, HR-like cell death (Fig. S9, see Supporting Information), although whether this is the effect of HrpN located in plant cells is unclear.

Three harpin-associated proteins have been reported in plants: AtHIPM, AtPIP1;4 and FIB4 (Li *et al.*, 2015; Oh and Beer, 2007; Song *et al.*, 2002). Among them, AtHIPM and AtPIP1;4 are involved in the mediation of enhanced plant growth on harpin treatment (Li *et al.*, 2015; Oh and Beer, 2007), whereas the function of FIB4 in harpin-mediated responses is ambiguous. FIB4, as a thylakoid membrane-localized protein, increases plant immunity and detoxifies redox in the chloroplast (Singh *et al.*, 2010). When treated with methyl viologen, which competes with Fd to accept electrons from PSI, the *FIB4*-knockdown apple mutant accumulates higher superoxide levels than WT (Singh *et al.*, 2010). The latter results, together with the current finding that Fd2 interacts with FIB4, suggest that FIB4 assists electron transport from photosynthesis to Fd. We therefore speculate that, when harpin is delivered into plant cells, it interacts with FIB4 and consequently disrupts Fd2 to receive electrons from photosynthesis, which is mediated by FIB4, ultimately leading to ROS accumulation in chloroplasts and cell death. However, more research is needed to clarify how Fd2 and FIB4 mediate plant responses to harpin.

Potential roles of Fd2 in the regulation of retrograde signalling

Activation of plant immunity depends on dramatic changes in the cellular redox status, which result in the reprogramming of the transcriptome and the establishment of both local and systemic defence (Spoel and Loake, 2011). In the stroma, Fd is the most upstream acceptor of electrons generated by photosynthesis, and Fd therefore determines the redox status of various downstream reductants, such as NADPH and thioredoxin (TRX) (Hanke and Mulo, 2013). To balance the redox outside of the chloroplast, NADPH-dependent thioredoxin reductases (NTRA and NTRB) are required to maintain the pool of reduced TRX in the cytoplasm (Sweat and Wolpert, 2007). By transferring electrons generated by PSI to $NADP^+$ via Fd, the chloroplast is the main NADPH-producing organelle. Therefore, deletion of Fd2 may disrupt the reduction of cytoplasmic TRX by decreasing the amount of available NADPH, which can further affect nuclear gene transcription (Tada *et al.*, 2008).

In addition, some plant transcription factors, such as TGA1 and TGA4 in Arabidopsis, rely on their oxidation state to regulate gene transcription (Després *et al.*, 2003). The reductant which regulates the redox status in the nucleus is still unknown. Stromules, emanated from plastid bodies, have been found recently to be involved in the chloroplast to nuclear transport of immunity signals (Caplan *et al.*, 2015). It is still unclear, however, how a protein can move from stromules to the nucleus across the inner and outer chloroplast membranes and to the nuclear envelope. According to our observations, Fd2 may be delivered from chloroplasts to the nucleus via stromules. This raises the possibility that Fd2 may be involved in retrograde chloroplast to nucleus signalling by reducing transcription factors in the nucleus. If this is correct, it is not surprising to find that the expression of many genes involved in the immune response, including genes regulating SA signalling and PTI, are regulated by Fd2.

EXPERIMENTAL PROCEDURES

Plant growth conditions

The Arabidopsis *Fd2–KO* mutant (Voss *et al.*, 2008) and the corresponding WT, Nossen, were kindly provided by Renate Scheibe's laboratory (University of Osnabrück, Germany) and by Hong-Bin Wang's laboratory (Sun Yat-sen University, China). Arabidopsis T-DNA insertion mutant *fib4-1* (SALK_014831) (Singh *et al.*, 2010) was obtained from the Arabidopsis Biological Resource Center (http://www.biosci.ohio-state.edu/pcmb/Facilities/abrc/abrchome.htm) (Alonso *et al.*, 2003). Arabidopsis plants were grown in a growth room at 20–22°C under a 10-h light/14-h dark cycle.

Pathogen infections

The powdery mildew pathogen *G. cichoracearum* (strain UCSC1) was maintained on the Arabidopsis *pad4-1* mutant. The inoculation method has been described previously (Shi *et al.*, 2013; Wang *et al.*, 2011). Trypan

blue staining was used to monitor fungal growth in the leaves at 8 dpi. Fungal growth and conidiation were quantified as described previously (Consonni *et al.*, 2006). *Pst* DC3000 infection by infiltration and a bacterial growth assay were performed as described previously (Geng *et al.*, 2012) with minor differences: 4-week-old plants were used for infiltration, and leaf discs were harvested at 3 dpi for analysis of bacterial growth.

ROS measurement

An oxidative burst assay was carried out as described previously (Zhang *et al.*, 2010) with minor modifications. The leaf strips were treated with 100 nM flg22 or 200 μg/mL chitin in 200 mL of buffer containing 20 μM luminol and 1 μg/mL horseradish peroxidase to immediately test the ROS burst. Each data point represented eight replicates.

DAB staining

To determine the accumulation of H_2O_2 after pathogen challenge, we stained the infected leaves with DAB. Four-week-old Nossen and *Fd2-KO* plants were spray inoculated with an avirulent isolate containing *avrRpt2*. Ten hours after inoculation, the infected leaves were cut and briefly washed with water. After the leaves had been stained with 0.1% (w/v) DAB overnight in the dark, they were destained with 95% ethanol and preserved in 50% ethanol. H_2O_2 production was indicated by a reddish-brown colour, and the relative DAB staining intensity was analysed by Image J.

Phytohormone quantification

Arabidopsis leaf samples were harvested at 2 dpi with *Pst* DC3000 or buffer and were flash frozen in liquid nitrogen. For phytohormone quantification, approximately 50 mg per sample was triple-ground in liquid nitrogen and placed in a tube. A 1-mL volume of 50 mM sodium phosphate buffer (pH 7.0) was added to each tube, and samples were extracted as described previously (Blakeslee and Murphy, 2016). The following were added to each tube as internal standards (ISTD): 12.5 ng of [$^2H_6$] (+)-*cis*,-*trans*-abscisic acid (d6-ABA, OlchemIm Ltd., Olomouc, Czech Republic, part #0342722); 5 ng of jasmonic-d5 acid (2,4,4-d3; acetyl-2,2-d2) (d5-JA, CDN Isotopes, Pointe-Claire, QC, Canada, part #D-6936); and 12.5 ng of 2-hydroxybenzoic acid-d6 (d6-SA, CDN Isotopes, part #D-1156). Samples were mixed with a vortex apparatus, extracted for 20 min at 4°C with gentle shaking on a nutator, and centrifuged at 12 000 ***g*** for 15 min at 4°C. Samples were separated using an Agilent Poroshell 120EC-C18 (3.5 × 50 mm^2, 2.7 μm) column and an acidified water–methanol buffer system (buffer A, 0.1% acetate, 5% methanol in water; buffer B, 0.1% acetate in methanol). Gradient conditions were as follows: 3 min 2%–50% B, 2 min 50%–98% B, hold at 98% B for 2 min, and then back to 2% B for 1 min. Eluted compounds were further separated and quantified using an Agilent 6460 triple quadrupole dual mass spectrometer equipped with an electrospray ionization source (ESI) (Agilent Technologies, Santa Clara, CA, USA). Compounds were quantified in negative ion mode, and mass transitions for each compound are provided in Table S3 (see Supporting Information). Compound identity was confirmed by comparing retention times and mass transitions with the authentic standards described above. Because of the transient nature of increases in phytohormone concentrations following stress stimuli, these experiments were repeated three times, with each experiment containing three to five biological replicates.

Quantitative real-time polymerase chain reaction (qRT-PCR)

Total RNAs were extracted from 100 mg of Arabidopsis leaf tissue using TRIzol reagent (Thermo Fisher Scientific, 15596, Waltham, MA , USA) following the manufacturer's instructions. A 3-μg quantity of total RNA was treated with DNase I (Invitrogen, 18068-015, Carlsbad, CA, USA) to remove DNA contamination, according to the manufacturer's instructions. The RNA samples were then subjected to first-strand cDNA synthesis using the Promega reverse transcription kit (Promega, A3500, Fitchburg, Wisconsin, USA) following the manufacturer's instructions. qRT-PCR was carried out using the CFX96 Touch Real-Time PCR Detection System (Bio-Rad, Hercules, California, USA). The qRT-PCR data were subjected to standard statistical analysis. Primers of the marker genes used in this study are listed in Table S2 (see Supporting Information).

Agrobacterium-mediated transient expression in *N. benthamiana*, plant protein extraction and immunoblotting

Agrobacterium GV3101 carrying the indicated plasmids was infiltrated into 5-week-old *N. benthamiana* leaves. All primers used for plasmid construction in this study are listed in Table S1 (see Supporting Information). The agroinfiltration assay in *N. benthamiana* was carried out as described previously (Park *et al.*, 2012). Total plant protein was extracted by grinding tissue in liquid nitrogen and immediately transferring the homogenate to 1 mL of extraction buffer containing 150 mM NaCl, 50 mM Tris-HCl, pH 7.6, 1 mM ethylenediaminetetraacetic acid (EDTA), 0.5% Triton X-100, 2 mM dithiothreitol (DTT) and plant protease inhibitor cocktail (Sigma-Aldrich, St. Louis, Missouri, USA). The samples were centrifuged at 16200 g for 15 min at 4°C, and the supernatant was used for immunoblotting as described previously (Park *et al.*, 2012).

Co-IP assay in *N. benthamiana*

For co-IP, 50 μL of a 50% slurry (v/v) of protein G-agarose beads (Roche, 11719416001, Pleasanton, CA, USA) was washed with 1 × phosphate-buffered saline (PBS) and then incubated with 5 μL of α-GFP antibody (Roche, 11814460001) at 4°C overnight with gentle rotation. Following centrifugation and removal of the buffer, protein samples (500 μL) were added to the beads with shaking for 6 h at 4°C. After the beads had been washed four times with washing buffer (150 mM NaCl, 50 mM Tris-HCl, pH 7.6, 1 mM EDTA, 0.3% Triton X-100 and 2 mM DTT), 50 μL of 1 × sodium dodecylsulfate (SDS) loading buffer was added, and the sample was heated to 95°C for 5 min. Then, 15 μL of each sample was loaded for gel running and immunoblotting with α-HA antibody (Roche, 1867423) or α-Myc antibody (Sigma-Aldrich, M4439).

GST pull-down

The target genes were cloned into pGEX 6p-1 and pMAL-c2x vectors to express proteins in *Escherichia coli* with N-terminus-fused GST and MBP

tags, respectively. The fusion proteins were prepared according to the manufacturer's instructions. The concentration of proteins in the supernatant was determined with the Bio-Rad protein assay reagent (500-0006). For the GST pull-down assay, about 5 μg of purified GST-fused proteins and GST were incubated with 40 μL of glutathione resin beads (GoldBio, G-250-100, St. Louis, MO, USA) for 4 h at 4°C with gentle shaking. After the supernatant had been removed and the pellet had been washed three times with PBS, 5 μg of purified MBP-fused proteins (purified with amylose resin, NEB E8021S, Ipswich, Massachusetts, UK, following the manufacturer's instructions) was added to the beads with end-over-end mixing for 6 h at 4°C. The beads were then washed four times with PBST buffer (1 × PBS with 0.5% Triton X-100 and 1 mM EDTA). Following centrifugation and removal of the supernatant, SDS loading buffer was added to the beads. The preparation was heated for 5 min before 15 μL of each sample was loaded for gel running. α-MBP (NEB, E8032S) and α-GST (Invitrogen, 71–7500) were used for immunoblot analysis.

Split-luciferase complementation assay

Fd2 was cloned into the pCAMBIA NLuc vector with the N-terminal half of luciferase (nLuc) using Gateway technology, resulting in Fd2-nLuc; FIB4 was cloned into the pCAMBIA CLuc vector with the C-terminal half of luciferase (cLuc), resulting in FIB4-cLuc (Chen *et al.*, 2008; Lee *et al.*, 2015). After individual transformation into *Agrobacterium* GV3101, they were transiently co-expressed in *N. benthamiana* leaves by infiltration with a final concentration of $OD_{600} = 0.6$ (OD_{600}, optical density at 600 nm) for each construct. On the same leaves, GV3101 carrying the empty nLuc vector and the FIB4-cLuc construct or the empty cLuc vector and the Fd2-nLuc construct was co-infiltrated as a control. Two days after inoculation, the inoculated leaves were sprayed with 1 mM luciferin, and chemiluminescence images were captured by ChemiDoc XRS+ (Bio-Rad). The fluorescence intensity was quantified with Image Lab 5.2 software.

Microscopic analysis

Protoplasts were isolated as described previously (Breuers *et al.*, 2012). Protoplasts were observed with a Nikon (Shinagawa, Tokyo, Japan) Eclipse 80i microscope and photographed with a Nikon DS-Qi1 camera. Plant tissues were observed with a Nikon A1 confocal microscope. Images were processed with NIS-Elements (Shinagawa, Tokyo, Japan) imaging software. To detect the GFP signal, 488 nm excitation and 507 nm detection wavelengths were used; to detect the chloroplast autofluorescence, 535 nm excitation and 620 nm detection wavelengths were used. For nuclear staining, 10 μg/mL of DAPI (Invitrogen, NL5995050) was used.

ACKNOWLEDGEMENTS

We thank R. Scheibe and H.-B. Wang for providing Nossen and *Fd2-KO* seeds. This work was supported by a grant from Plant Health Care Inc. (Grant No. #1000).

REFERENCES

Akamatsu, A., Wong, H.L., Fujiwara, M., Okuda, J., Nishide, K., Uno, K., Imai, K., Umemura, K., Kawasaki, T., Kawano, Y.. and Shimamoto, K. (2013) An OsCEBiP/OsCERK1-OsRacGEF1-OsRac1 module is an essential early component of chitin-induced rice immunity. *Cell Host Microbe*, **13**, 465–476.

Alonso, J.M., Stepanova, A.N., Leisse, T.J., Kim, C.J., Chen, H. and Shinn, P. (2003) Genome-wide insertional mutagenesis of *Arabidopsis thaliana*. *Science*, **301**, 653–657.

Asai, T., Tena, G., Plotnikova, J., Willmann, M.R., Chiu, W.-L., Gomez-Gomez, L., Boller, T., Ausubel, F.M. and Sheen, J. (2002) MAP kinase signalling cascade in Arabidopsis innate immunity. *Nature*, **415**, 977–983.

Axtell, M.J. and Staskawicz, B.J. (2003) Initiation of RPS2-specified disease resistance in Arabidopsis is coupled to the AvrRpt2-directed elimination of RIN4. *Cell*, **112**, 369–377.

Bari, R. and Jones, J.D.G. (2009) Role of plant hormones in plant defence responses. *Plant Mol. Biol.* **69**, 473–488.

Blakeslee, J.J. and Murphy, A.S. (2016) Microscopic and biochemical visualization of auxins in plant tissues. In: *Environmental Responses in Plants: Methods and Protocols* (Duque, P., ed.), pp. 37–53. New York, NY: Springer.

Boccara, M., Schwartz, W., Guiot, E., Vidal, G., De Paepe, R., Dubois, A.. and Boccara, A.-C. (2007) Early chloroplastic alterations analysed by optical coherence tomography during a harpin-induced hypersensitive response. *Plant J.* **50**, 338–346.

Bocsanczy, A.M., Nissinen, R.M., Oh, C. and Beer, S.V. (2008) HrpN of *Erwinia amylovora* functions in the translocation of DspA/E into plant cells. *Mol. Plant Pathol.* **9**, 425–434.

Breuers, F.K., Bräutigam, A., Geimer, S., Welzel, U.Y., Stefano, G., Renna, L., Brandizzi, F. and Weber, A.P. (2012) Dynamic remodeling of the plastid envelope membranes—a tool for chloroplast envelope in vivo localizations. *Front. Plant Sci.* **3**, 7.

Caplan, J.L., Kumar, A.S., Park, E., Padmanabhan, M.S., Hoban, K., Modla, S., Czymmek, K. and Dinesh-Kumar, S.P. (2015) Chloroplast stromules function during innate immunity. *Dev. Cell*, **34**, 45–57.

Chen, H., Zou, Y., Shang, Y., Lin, H., Wang, Y., Cai, R., Tang, X. and Zhou, J.-M. (2008) Firefly luciferase complementation imaging assay for protein–protein interactions in plants. *Plant Physiol.* **146**, 368–376.

Chisholm, S.T., Coaker, G., Day, B. and Staskawicz, B.J. (2006) Host–microbe interactions: shaping the evolution of the plant immune response. *Cell*, **124**, 803–814.

Choi, M.-S., Kim, W., Lee, C. and Oh, C.-S. (2013) Harpins, multifunctional proteins secreted by Gram-negative plant-pathogenic bacteria. *Mol. Plant–Microbe Interact.* **26**, 1115–1122.

Clarke, J.D., Volko, S.M., Ledford, H., Ausubel, F.M. and Dong, X. (2000) Roles of salicylic acid, jasmonic acid, and ethylene in cpr-induced resistance in Arabidopsis. *Plant Cell*, **12**, 2175–2190.

Consonni, C., Humphry, M.E., Hartmann, H.A., Livaja, M., Durner, J., Westphal, L., Vogel, J., Lipka, V., Kemmerling, B., Schulze-Lefert, P., Somerville, S.C. and Panstruga, R. (2006) Conserved requirement for a plant host cell protein in powdery mildew pathogenesis. *Nat. Genet.* **38**, 716–720.

Dayakar, B.V., Lin, H.-J., Chen, C.-H., Ger, M.-J., Lee, B.-H., Pai, C.-H., Chow, D., Huang, H.E., Hwang, S.Y., Chung, M.C. and Feng, T.Y. (2003) Ferredoxin from sweet pepper (*Capsicum annuum* L.) intensifying harpin pss-mediated hypersensitive response shows an enhanced production of active oxygen species (AOS). *Plant Mol. Biol.* **51**, 913–924.

Demmig-Adams, B., Cohu, C.M., Amiard, V., van Zadelhoff, G., Veldink, G.A., Muller, O. and Adams, W.W. (2013) Emerging trade-offs—impact of photoprotectants (PsbS, xanthophylls, and vitamin E) on oxylipins as regulators of development and defense. *New Phytol.* **197**, 720–729.

Després, C., Chubak, C., Rochon, A., Clark, R., Bethune, T., Desveaux, D. and Fobert, P.R. (2003) The Arabidopsis NPR1 disease resistance protein is a novel cofactor that confers redox regulation of DNA binding activity to the basic domain/leucine zipper transcription factor TGA1. *Plant Cell*, **15**, 2181–2191.

Friso, G., Giacomelli, L., Ytterberg, A.J., Peltier, J.-B., Rudella, A., Sun, Q. and Wijk, K.J. (2004) In-depth analysis of the thylakoid membrane proteome of *Arabidopsis thaliana* chloroplasts: new proteins, new functions, and a plastid proteome database. *Plant Cell*, **16**, 478–499.

Galetskiy, D., Susnea, I., Reiser, V., Adamska, I. and Przybylski, M. (2008) Structure and dynamics of photosystem II light-harvesting complex revealed by high-resolution FTICR mass spectrometric proteome analysis. *J. Am. Soc. Mass Spectrom.* **19**, 1004–1013.

Geng, X., Cheng, J., Gangadharan, A. and Mackey, D. (2012) The coronatine toxin of *Pseudomonas syringae* is a multifunctional suppressor of Arabidopsis defense. *Plant Cell*, **24**, 4763–4774.

Ger, M.-J., Louh, G.-Y., Lin, Y.-H., Feng, T.-Y. and Huang, H.-E. (2014) Ectopically expressed sweet pepper ferredoxin PFLP enhances disease resistance to

Pectobacterium carotovorum subsp. *carotovorum* affected by harpin and protease-mediated hypersensitive response in Arabidopsis. *Mol. Plant Pathol.* **15**, 892–906.

Glazebrook, J. (2005) Contrasting mechanisms of defense against biotrophic and necrotrophic pathogens. *Annu. Rev. Phytopathol.* **43**, 205–227.

Hanke, G.T. and Hase, T. (2008) Variable photosynthetic roles of two leaf-type ferredoxins in Arabidopsis, as revealed by RNA interference. *Photochem Photobiol.* **84**, 1302–1309.

Hanke, G.T. and Mulo, P. (2013) Plant type ferredoxins and ferredoxin-dependent metabolism. *Plant Cell Environ.* **36**, 1071–1084.

Hanke, G.T., Kimata-Ariga, Y., Taniguchi, I. and Hase, T. (2004) A post genomic characterization of Arabidopsis ferredoxins. *Plant Physiol.* **134**, 255–264.

Howe, G.A. and Schilmiller, A.L. (2002) Oxylipin metabolism in response to stress. *Curr. Opin. Plant Biol.* **5**, 230–236.

Ishiga, Y., Ishiga, T., Ikeda, Y., Matsuura, T. and Mysore, K.S. (2016) NADPH-dependent thioredoxin reductase C plays a role in nonhost disease resistance against *Pseudomonas syringae* pathogens by regulating chloroplast-generated reactive oxygen species. *PeerJ.* **4**, e1938.

Jones, J.D.G. and Dangl, J.L. (2006) The plant immune system. *Nature*, **444**, 323–329.

Lee, D., Bourdais, G., Yu, G., Robatzek, S. and Coaker, G. (2015) Phosphorylation of the plant immune regulator RPM1-INTERACTING PROTEIN4 enhances plant plasma membrane H+-ATPase activity and inhibits flagellin-triggered immune responses in Arabidopsis. *Plant Cell*, **27**, 2042–2056.

Li, L., Wang, H., Gago, J., Cui, H., Qian, Z., Kodama, N., Ji, H., Tian, S., Shen, D., Chen, Y., Sun, F., Xia, Z., Ye, Q., Sun, W., Flexas, J. and Dong, H. (2015) Harpin Hpa1 interacts with aquaporin PIP1;4 to promote the substrate transport and photosynthesis in Arabidopsis. *Sci. Rep.* **5**, 17 207. doi:10.1038/srep17207

Liu, J., Wang, P., Liu, B., Feng, D., Zhang, J., Su, J., Zhang, Y., Wang, J.F. and Wang, H.B. (2013) A deficiency in chloroplastic ferredoxin 2 facilitates effective photosynthetic capacity during long-term high light acclimation in *Arabidopsis thaliana*. *Plant J.* **76**, 861–874.

Liu, L., Sonbol, F.-M., Huot, B., Gu, Y., Withers, J., Mwimba, M., Yao, J., He, S.Y. and Dong, X. (2016) Salicylic acid receptors activate jasmonic acid signalling through a non-canonical pathway to promote effector-triggered immunity. *Nat. Commun.* **7**, 13 099.

Liu, W., Liu, J., Ning, Y., Ding, B., Wang, X., Wang, Z. and Wang, G.L. (2013) Recent progress in understanding PAMP- and effector-triggered immunity against the rice blast fungus *Magnaporthe oryzae*. *Mol. Plant.* **6**, 605–620.

Lorenzo, O., Chico, J.M., Sánchez-Serrano, J.J. and Solano, R. (2004) JASMONATE-INSENSITIVE1 encodes a MYC transcription factor essential to discriminate between different jasmonate-regulated defense responses in Arabidopsis. *Plant Cell*, **16**, 1938–1950.

Mackey, D., Holt, B.F., Wiig, A. and Dangl, L., J. (2002) RIN4 interacts with type III effector molecules and is required for RPM1-mediated resistance in Arabidopsis. *Curr. Biol.* **108**, 743–754.

Mur, L.A.J., Aubry, S., Mondhe, M., Kingston-Smith, A., Gallagher, J., Timms-Taravella, E., James, C., Papp, I., Hörtensteiner, S., Thomas, H. and Ougham, H. (2010) Accumulation of chlorophyll catabolites photosensitizes the hypersensitive response elicited by *Pseudomonas syringae* in Arabidopsis. *New Phytol.* **188**, 161–174.

Nomura, H., Komori, T., Uemura, S., Kanda, Y., Shimotani, K., Nakai, K., Furuichi, T., Takebayashi, K., Sugimoto, T., Sano, S., Suwastika, I.N, Fukusaki, E., Yoshioka, H., Nakahira, Y. and Shiina, T. (2012) Chloroplast-mediated activation of plant immune signalling in Arabidopsis. *Nat. Commun.* **3**, 926.

Oh, C.-S. and Beer, S.V. (2007) AtHIPM, an ortholog of the apple HrpN-interacting protein, is a negative regulator of plant growth and mediates the growth-enhancing effect of HrpN in Arabidopsis. *Plant Physiol.* **145**, 426–436.

Padmanabhan, M.S. and Dinesh-Kumar, S.P. (2010) All hands on deck—the role of chloroplasts, endoplasmic reticulum, and the nucleus in driving plant innate immunity. *Mol. Plant–Microbe Interact.* **23**, 1368–1380.

Park, C.-H., Chen, S., Shirsekar, G., Zhou, B., Khang, C.H., Songkumarn, P., Afzal, A.J., Ning, Y., Wang, R., Bellizzi, M., Valent, B. and Wang, G.-L. (2012) The *Magnaporthe oryzae* effector AvrPiz-t targets the RING E3 Ubiquitin Ligase APIP6 to suppress pathogen-associated molecular pattern-triggered immunity in rice. *Plant Cell*, **24**, 4748–4762.

Peltier, J.-B., Ytterberg, A.J., Sun, Q. and van Wijk, K.J. (2004) New functions of the thylakoid membrane proteome of *Arabidopsis thaliana* revealed by a simple, fast, and versatile fractionation strategy. *J. Biol. Chem.* **279**, 49 367–49 383.

Penninckx, I.A., Thomma, B.P., Buchala, A., Métraux, J.P. and Broekaert, W.F. (1998) Concomitant activation of jasmonate and ethylene response pathways is required for induction of a plant defensin gene in Arabidopsis. *Plant Cell*, **10**, 2103–2113.

Schwessinger, B. and Ronald, P.C. (2012) Plant innate immunity: perception of conserved microbial signatures. *Annu. Rev. Plant Biol.* **63**, 451–482.

Serrano, I., Audran, C. and Rivas, S. (2016) Chloroplasts at work during plant innate immunity. *J Exp Bot.* **67**, 3845–3854.

Serrano, M., Wang, B., Aryal, B., Garcion, C., Abou-Mansour, E., Heck, S., Geisler, M., Mauch, F., Nawrath, C. and Métraux, J.-P. (2013) Export of salicylic acid from the chloroplast requires the multidrug and toxin extrusion-like transporter EDS5. *Plant Physiol.* **162**, 1815–1821.

Shapiguzov, A., Vainonen, J.P., Wrzaczek, M. and Kangasjärvi, J. (2012) ROS-talk – how the apoplast, the chloroplast, and the nucleus get the message through. *Front. Plant Sci.* **3**, 292.

Shi, H., Shen, Q., Qi, Y., Yan, H., Nie, H., Chen, Y., Zhao, T., Katagiri, F. and Tang, D. (2013) BR-SIGNALING KINASE1 physically associates with FLAGELLIN SENSING2 and regulates plant innate immunity in Arabidopsis. *Plant Cell*, **25**, 1143–1157.

Singh, D.K., Maximova, S.N., Jensen, P.J., Lehman, B.L., Ngugi, H.K. and McNellis, T.W. (2010) FIBRILLIN4 is required for plastoglobule development and stress resistance in apple and Arabidopsis. *Plant Physiol.* **154**, 1281–1293.

Singh, D.K., Laremore, T.N., Smith, P.B., Maximova, S.N. and McNellis, T.W. (2012) Knockdown of FIBRILLIN4 gene expression in apple decreases plastoglobule plastoquinone content. *PLoS One*, **7**, e47547.

Song, X., Bariola, P., Linderoth, N., Fan, H. and Wei, Z.-M. (2002) *Receptors for hypersensitive response elicitors and uses thereof*. US Patent Application No. 20020007501.

Spoel, S.H. and Loake, G.J. (2011) Redox-based protein modifications: the missing link in plant immune signalling. *Curr. Opin. Plant Biol.* **14**, 358–364.

Stael, S., Kmiecik, P., Willems, P., Van Der Kelen, K., Coll, N.S., Teige, M. and Van Breusegem, F. (2015) Plant innate immunity–sunny side up? *Trends Plant Sci.* **20**, 3.

Sweat, T.A. and Wolpert, T.J. (2007) Thioredoxin h5 is required for victorin sensitivity mediated by a CC-NBS-LRR gene in Arabidopsis. *Plant Cell*, **19**, 673–687.

Tada, Y., Spoel, S.H., Pajerowska-Mukhtar, K., Mou, Z., Song, J., Wang, C., Zuo, J. and Dong, X. (2008) Plant immunity requires conformational charges of NPR1 via S-nitrosylation and thioredoxins. *Science*, **321**, 952–956.

Tao, Y., Xie, Z., Chen, W., Glazebrook, J., Chang, H.-S. and Han, B. (2003) Quantitative nature of Arabidopsis responses during compatible and incompatible interactions with the bacterial pathogen *Pseudomonas syringae*. *Plant Cell*, **15**, 317–330.

Thaler, J.S., Humphrey, P.T. and Whiteman, N.K. (2012) Evolution of jasmonate and salicylate signal crosstalk. *Trends Plant Sci.* **17**, 260–270.

Torres, M.A., Dangl, J.L. and Jones, J.D.G. (2002) Arabidopsis gp91phox homologues AtrbohD and AtrbohF are required for accumulation of reactive oxygen intermediates in the plant defense response. *Proc. Natl. Acad. Sci. USA*, **99**, 517–522.

de Torres Zabala, M., Littlejohn, G., Jayaraman, S., Studholme, D., Bailey, T., Lawson, T., Tillich, M., Licht, D., Bölter, B., Delfino, L., Truman, W., Mansfield, J., Smirnoff, N. and Grant, M. (2015) Chloroplasts play a central role in plant defence and are targeted by pathogen effectors. *Nat. Plants*, **1**, 15 074.

Vidi, P.-A., Kanwischer, M., Baginsky, S., Austin, J.R., Csucs, G., Dörmann, P., Kessler, F. and Bréhélin, C. (2006) Tocopherol cyclase (VTE1) localization and vitamin E accumulation in chloroplast plastoglobule lipoprotein particles. *J. Biol. Chem.* **281**, 11 225–11 234.

Vlot, A.C., Dempsey, D.M.A. and Klessig, D.F. (2009) Salicylic acid, a multifaceted hormone to combat disease. *Annu. Rev. Phytopathol.* **47**, 177–206.

Voss, I., Koelmann, M., Wojtera, J., Holtgrefe, S., Kitzmann, C., Backhausen, J.E. and Scheibe, R. (2008) Knockout of major leaf ferredoxin reveals new redox-regulatory adaptations in *Arabidopsis thaliana*. *Physiol. Plant.* **133**, 584–598.

Wang, Y., Nishimura, M.T., Zhao, T. and Tang, D. (2011) ATG2, an autophagy-related protein, negatively affects powdery mildew resistance and mildew-induced cell death in Arabidopsis. *Plant J.* **68**, 74–87.

Wasternack, C. and Hause, B. (2013) Jasmonates: biosynthesis, perception, signal transduction and action in plant stress response, growth and development. An update to the 2007 review in Annals of Botany. *Ann. Bot.* **111**, 1021–1058.

Wei, Z., Laby, R., Zumoff, C., Bauer, D., He, S., Collmer, A. and Beer, S. (1992) Harpin, elicitor of the hypersensitive response produced by the plant pathogen *Erwinia amylovora*. *Science*, **257**, 85–88.

Wildermuth, M.C., Dewdney, J., Wu, G. and Ausubel, F.M. (2001) Isochorismate synthase is required to synthesize salicylic acid for plant defence. *Nature*, **414**, 562–565.

Yamaguchi, K., Yamada, K., Ishikawa, K., Yoshimura, S., Hayashi, N., Uchihashi, K., Ishihama, N., Kishi-Kaboshi, M., Takahashi, A., Tsuge, S.,

Ochiai, H., Tada, Y., Shimamoto, K., Yoshioka, H. and Kawasaki, T. (2013) A receptor-like cytoplasmic kinase targeted by a plant pathogen effector is directly phosphorylated by the chitin receptor and mediates rice immunity. *Cell Host Microbe*, **13**, 347–357.

Yamamoto, H., Kato, H., Shinzaki, Y., Horiguchi, S., Shikanai, T., Hase, T., Endo, T., Nishioka, M., Makino, A., Tomizawa, K. and Miyake, C. (2006) Ferredoxin limits cyclic electron flow around PSI (CEF-PSI) in higher plants—stimulation of CEF-PSI enhances non-photochemical quenching of Chl fluorescence in transplastomic tobacco. *Plant Cell Physiol.* **47**, 1355–1371.

Ytterberg, A.J., Peltier, J.-B. and Van Wijk, K.J. (2006) Protein profiling of plastoglobules in chloroplasts and chromoplasts. A surprising site for differential accumulation of metabolic enzymes. *Plant Physiol.* **140**, 984–997.

Zhang, J., Li, W., Xiang, T., Liu, Z., Laluk, K., Ding, X., Zou, Y., Gao, M., Zhang, X., Chen, S., Mengiste, T., Zhang, Y. and Zhou, J.-M. (2010) Receptor-like cytoplasmic kinases integrate signaling from multiple plant immune receptors and are targeted by a *Pseudomonas syringae* effector. *Cell Host Microbe*, **7**, 290–301.

Zhang, Y., Fan, W., Kinkema, M., Li, X. and Dong, X. (1999) Interaction of NPR1 with basic leucine zipper protein transcription factors that bind sequences required for salicylic acid induction of the PR-1 gene. *Proc. Natl. Acad. Sci. USA*, **96**, 6523–6528.

Zheng, X.-Y, Spivey, N.W., Zeng, W., Liu, P.-P., Fu, Z.Q., Klessig, D.F., He, S.Y. and Dong, X. (2012) Coronatine promotes *Pseudomonas syringae* virulence in plants by activating a signaling cascade that inhibits salicylic acid accumulation. *Cell Host Microbe*, **11**, 587–596.

SUPPORTING INFORMATION

Additional Supporting Information may be found in the online version of this article at the publisher's website:

Fig. S1 The expression of Fd2 is reduced by *Pseudomonas syringae* pv. *tomato* (*Pst*) DC3000. (a) Total protein was extracted from Col-0 before and at 2 days after *Pst* DC3000 infiltration. The protein level of Fd2 was determined by western blot using antiserum against ferredoxin in *Spinacia oleracea* (FDX1, top line) with Ponceau S staining of input Rubisco as the loading control (bottom line). (b) The relative intensity of immunoblotting bands is shown. Error bars represent the standard error (SE) ($n = 3$) from three biological repeats, and significance was determined at $*P < 0.05$ with Student's *t*-test. dpi, days post-infection.

Fig. S2 The transcriptional levels of *NPR1* (a) and *EDS5* (b) in Nossen and *Fd2-KO* before and after *Pseudomonas syringae* pv. *tomato* (*Pst*) DC3000 [optical density at 600 nm (OD_{600}) = 0.0002] infection. Quantitative real-time polymerase chain reaction (qRT-PCR) was carried out with *Actin* as the endogenous control. Significance was determined at $*P < 0.05$ and $**P < 0.01$ with Student's *t*-test. Error bars represent the standard error (SE) ($n = 3$). Experiments were conducted in triplicate with similar results. dpi, days post-infection.

Fig. S3 Protein levels of FIB4-cLuc in *Nicotiana benthamiana* leaves transiently expressing split-luciferase complementation vectors. Immunoblotting was carried out with the anti-cLuc antibody.

Fig. S4 FIBRILLIN4 (FIB4) binds to HrpN. (a) FIB4 interacts with HrpN as indicated by a pull-down assay. Purified GST-HrpN and glutathione *S*-transferase (GST) were bound to glutathione resin beads and incubated with purified maltose-binding protein (MBP)-FIB4. After the preparation had been washed, the *in vitro* interaction of MBP-FIB4 with GST-HrpN was detected by western blotting with α-MBP antibody (top); 30% of the input was loaded and the sample amounts were shown by Coomassie blue staining (bottom). (b) FIB4 interacts with HrpN as indicated by co-immunoprecipitation (co-IP). FIB4-GFP and Myc-HrpN were co-expressed in *Nicotiana benthamiana* by agroinfiltration, with Myc-HrpN expressed alone as the control. Proteins were extracted 3 days after infiltration, and immunoprecipitation was carried out with anti-green fluorescent protein (anti-GFP) antibody (top). The input is shown at the bottom.

Fig. S5 The transcript analysis of *FIB4* (a) and *Fd2* (b) in *Fd2-KO* and *fib4-1*, respectively, relative to the wild-types. *FIB4* transcription was suppressed in *Fd2-KO*, whereas *Fd2* was induced in *fib4-1. Actin* was used as the endogenous control. Significance was determined at $**P < 0.01$ with Student's *t*-test. Error bars represent the standard error (SE) ($n = 3$). Experiments were conducted in triplicate with similar results.

Fig. S6 Both *Fd2* and *FIB4* are harpin-responsive genes. Four-week-old Col-0 plants were sprayed with 5 μg/mL glutathione *S*-transferase (GST) and GST-HrpN. Leaf tissues were harvested at the indicated times for analysis of the relative transcript levels of *Fd2* (a) and *FIB4* (b). Compared with the GST control, both *Fd2* and *FIB4* were up-regulated by HrpN treatment. *Actin* was used as the endogenous control; error bars represent the standard error (SE) ($n = 3$); significance was determined at $**P < 0.01$ with Student's *t*-test. Experiments were conducted in triplicate with similar results.

Fig. S7 Both FIBRILLIN4 (FIB4) and Fd2 are localized to chloroplasts. Protoplasts were prepared from *Nicotiana benthamiana* leaves transiently expressing FIB4-GFP or Fd2-GFP by agroinfiltration. Both Fd2-GFP and FIB4-GFP (green) localize to chloroplasts (red, autofluorescence). Bars, 10 μm.

Fig. S8 Immunoblotting to detect Fd2-GFP transiently expressed in *Nicotiana benthamiana* leaves. Fd2-GFP was transiently expressed in *N. benthamiana* by agroinfiltration. Total protein was extracted 3 days after infiltration, and western blot was carried out with anti-green fluorescent protein (anti-GFP) antibody.

Fig. S9 Transient expression of HrpN in *Nicotiana benthamiana* caused weak cell death. At 3 days after transient expression of HrpN-GFP by agroinfiltration, a weak, hypersensitive response (HR)-like cell death was observed on the leaf. The leaf expressing Fd2-GFP was used as a control. Bars, 5 mm.

Table S1 Primers used for plasmid construction.

Table S2 Primers used for real-time polymerase chain reaction (PCR) analysis.

Table S3 Tandem mass spectroscopy (MS/MS) settings and mass transition used to quantify salicylic acid (SA), jasmonic acid (JA) and JA-isoleucine/leucine (JA-Ile/Leu).